

Disentangling SMEFT and UV contributions in $h \rightarrow Z\gamma$ and $h \rightarrow \gamma\gamma$ decays

KOSTAS MANTZAROPOULOS¹

¹*Department of Physics, University of Ioannina, GR 45 110, Greece*

July 15, 2024

Abstract

LHC searches have revealed that the Higgs boson decay to a photon pair is nearly consistent with the Standard Model (SM), whereas recently, there is evidence for the decay of the Higgs boson to a Z -boson and a photon. These decays are governed by the same set of Wilson-coefficients at the tree level in Standard Model Effective Field Theory (SMEFT). In this study, we aim to explain this potential discrepancy between the decays $h \rightarrow \gamma\gamma$ and $h \rightarrow Z\gamma$. We conduct a model-independent analysis in SMEFT to determine the magnitude and features of the Wilson coefficients required to account for the observed distinction between the two signal strengths. Following this, we adopt a top-down approach, considering all single and two field extensions of the SM, including scalars and fermions, as candidates for new interactions. We perform the matching of these models to one loop using automated packages and compare the models' predictions regarding $h \rightarrow Z\gamma$.

1 Introduction

Since the discovery of the Higgs particle by the LHC [1, 2] and the absence of any new smoking gun event our attention is turning more and more to studying in detail the properties and the couplings of the Higgs particle. Its decay and production can be affected by particles that have not yet been discovered or hinted at and are thus elusive. If these new particles are heavy the Standard Model Effective Field Theory (SMEFT) (for reviews we refer the reader to Refs. [3–5]) provides a framework to study the effects of particles that are found above the electroweak (EW) scale, namely $v \sim 245\text{GeV}$. The constituents of this framework are higher dimensional operators that respect the SM gauge group, for that we add to the SM Lagrangian the sum of terms with mass dimension greater than 4,

$$\mathcal{L} = \mathcal{L}_{\text{SM}} + \frac{C^5 \mathcal{O}^5}{\Lambda} + \frac{C^6 \mathcal{O}^6}{\Lambda^2} + \dots, \quad (1.1)$$

where as a superscript the mass dimension of each respective operator is denoted and Λ serves as the scale of new (UV) physics. Each operator is accompanied by its respective coefficient known as Wilson coefficient (W_c) whose expressions encode the effect of UV physics.

Deviations from the SM values of decay and production channels are encoded in the so called signal strength. These are calculated as the ratio,

$$\mu_{h \rightarrow X} = \frac{\Gamma(\text{SMEFT}, h \rightarrow X)}{\Gamma(\text{SM}, h \rightarrow X)} = 1 + \frac{\Gamma(\text{BSM}, h \rightarrow X)}{\Gamma(\text{SM}, h \rightarrow X)}, \quad (1.2)$$

where with $\Gamma(\text{BSM})$ we denote the decay rate that is affected only by physics beyond the SM (BSM). Hence new physics that contribute to each respective channel would shift $\mu_{h \rightarrow X}$ to values different than one. The decays of the Higgs into two bosons have been measured with high precision and in agreement with the SM are WW^* , ZZ^* , $\gamma\gamma$ [6–12]. A detailed analysis of the properties, the decay

and production as well as future directions for Higgs physics can be found in [13, 14]. Although most of the above decays are in agreement with the SM a recent analysis by the ATLAS and the CMS collaboration [15] found evidence for the decay of $h \rightarrow Z\gamma$, which was an elusive decay up to now. Additionally, they reported a mild excess of around $\sim 2\sigma$ with respect to the SM value, the measured signal strength is,

$$\mu_{h \rightarrow Z\gamma} = 2.2 \pm 0.7. \quad (1.3)$$

This means that new physics contributions have to account for $\mu_{h \rightarrow Z\gamma}^{\text{BSM}} = 1.2 \pm 0.7$, if we assume that all uncertainties come from the UV. This study aims to answer this question, which UV model could account for such an excess in the $h \rightarrow Z\gamma$ decay? The answer of course lies in the values of the Wcs that are found in the SMEFT. A few recent articles have tried to address this question varying the field content or extending the gauge group of the SM [16–19]. Another interesting article explores enhancements of $h \rightarrow Z\gamma$ through renormalization group effects of tree-level generated dimension 8 operators including also massive vector-boson fields [20], which are not considered in this work. Additionally, contributions from the MSSM in the $h \rightarrow Z\gamma$ can be found in the ref. [21].

The values of the Wcs that can affect the properties of the Higgs particle can be calculated by the process known as matching. In the matching procedure (top-down approach) Wcs are calculated through a complete UV model and their analytic expressions depend on the coupling of the UV model as well as the various scales (or scale). This procedure can be done either diagrammatically, or directly through the path integral. Each respective approach carries advantages as well as disadvantages. Functional matching since its inception [22, 23] has recently seen renowned interest with new techniques [24, 25] and universal results making their appearance [26–34], even at two-loop order [35]. The automation of all these techniques have been ranging from SuperTrace calculations [36, 37] all the way to quickly and easily calculating Wcs (at tree and loop level) from the Lagrangian [38–42].

Another approach to determining the effect of new physics on observables is the bottom-up approach. This is a model-agnostic method where the Wcs remain unknown and their value is determined by fitting a set of observables to a set of coefficients. Throughout this article we will be using the Warsaw basis [43] to study the effects of UV independent Wcs to the relevant decays of the Higgs boson. This allows us to gauge the magnitude of new physics that may affect each Wc respectively and may give us hints about the structure of the UV model. However the downside of this approach is the unknown correlations between Wcs that may arise from the UV model, so the bottom-up and the top-down approach should be seen as complementary to each other. One may give hints on high-scale physics while the other will pin down the correlations of Wcs and restrict the available space of Wcs since the couplings in the UV will be less than the independent Wcs in the Warsaw basis.

The structure of the paper is the following. In Section 2 we study the Higgs decays $h \rightarrow \gamma\gamma$ and $h \rightarrow Z\gamma$ at one-loop order, in the bottom-up approach, in the context of SMEFT. We make several rescalings to Wcs in order to account for their tree and one-loop level counterparts. After clearing up major contributions to their signal strengths we fit all Wcs to a set of observables related to the Higgs sector and compare the values of Wcs needed to account for their observed values. In Section 3, we turn our attention to possible UV complete models that may account for the values of Wcs found in the fit. All colorless single field extensions of the SM, that respect the gauge group, tabulated in the tree-level dictionary [44], are considered. In Section 4, we categorize interactions with respect to their loop functions and devise a scheme to tabulate two-filed models that generate Wcs relevant to the Higgs decays. We match all models to the Warsaw basis through automated packages and perform a constrained minimization to find the best values for the couplings and masses of each respective model. We leave the signal strength of the decay $h \rightarrow Z\gamma$ as a prediction of the model and plot the values for each one compared to $h \rightarrow \gamma\gamma$.

2 Model independent analysis in SMEFT

There are two Higgs decays in SMEFT that are of interest to us currently, namely, $h \rightarrow \gamma\gamma$ and $h \rightarrow Z\gamma$. Their semi-numerical expressions, at one-loop order, of the signal strengths, in the input scheme $\{G_F, M_W, M_Z\}$, and in units of TeV^{-2} , are [45, 46],

$$\begin{aligned} \delta R_{h \rightarrow Z\gamma} \simeq & 0.18 \left(C_{1221}^{\ell\ell} - C_{11}^{\phi\ell(3)} - C_{22}^{\phi\ell(3)} \right) + 0.12 \left(C^{\phi\square} - C^{\phi D} \right) \\ & - 0.01 \left(C_{33}^{d\phi} - C_{33}^{u\phi} \right) + 0.02 \left(C_{33}^{\phi u} + C_{33}^{\phi q(1)} - C_{33}^{\phi q(3)} \right) \\ & + \left[14.99 - 0.35 \log \frac{\mu^2}{M_W^2} \right] C^{\phi B} - \left[14.88 - 0.15 \log \frac{\mu^2}{M_W^2} \right] C^{\phi W} + \left[9.44 - 0.26 \log \frac{\mu^2}{M_W^2} \right] C^{\phi WB} \\ & + \left[0.10 - 0.20 \log \frac{\mu^2}{M_W^2} \right] C^W - \left[0.11 - 0.04 \log \frac{\mu^2}{M_W^2} \right] C_{33}^{uB} + \left[0.71 - 0.28 \log \frac{\mu^2}{M_W^2} \right] C_{33}^{uW} \\ & - 0.01 C_{22}^{uW} - 0.01 C_{33}^{dW} + \dots, \end{aligned} \quad (2.1)$$

$$\begin{aligned} \delta R_{h \rightarrow \gamma\gamma} \simeq & 0.18 \left(C_{1221}^{\ell\ell} - C_{11}^{\phi\ell(3)} - C_{22}^{\phi\ell(3)} \right) + 0.12 \left(C^{\phi\square} - 2C^{\phi D} \right) \\ & - 0.01 \left(C_{22}^{e\phi} + 4C_{33}^{e\phi} + 5C_{22}^{u\phi} + 2C_{33}^{d\phi} - 3C_{33}^{u\phi} \right) \\ & - \left[48.04 - 1.07 \log \frac{\mu^2}{M_W^2} \right] C^{\phi B} - \left[14.29 - 0.12 \log \frac{\mu^2}{M_W^2} \right] C^{\phi W} + \left[26.17 - 0.52 \log \frac{\mu^2}{M_W^2} \right] C^{\phi WB} \\ & + \left[0.16 - 0.22 \log \frac{\mu^2}{M_W^2} \right] C^W + \left[2.11 - 0.84 \log \frac{\mu^2}{M_W^2} \right] C_{33}^{uB} + \left[1.13 - 0.45 \log \frac{\mu^2}{M_W^2} \right] C_{33}^{uW} \\ & - \left[0.03 - 0.01 \log \frac{\mu^2}{M_W^2} \right] C_{22}^{uB} - \left[0.01 - 0.00 \log \frac{\mu^2}{M_W^2} \right] C_{22}^{uW} + \left[0.03 - 0.01 \log \frac{\mu^2}{M_W^2} \right] C_{33}^{dB} \\ & - \left[0.02 - 0.01 \log \frac{\mu^2}{M_W^2} \right] C_{33}^{dW} + \left[0.02 - 0.00 \log \frac{\mu^2}{M_W^2} \right] C_{33}^{eB} - \left[0.01 - 0.00 \log \frac{\mu^2}{M_W^2} \right] C_{33}^{eW} + \dots, \end{aligned} \quad (2.2)$$

where the dots denote terms whose contributions are lower than $0.01 \times C$ and μ is the renormalization scale. We are restricting ourselves to contributions without CP-violation. These operators are heavily constrained by Electric Dipole Moments (EDMs), and would contribute with tiny corrections to the observables and the problem we are trying to tackle in this work.

At a first glance we can naively say that the main contributions in these two observables come from the same three operators,

$$C^{\phi B}, \quad C^{\phi W}, \quad C^{\phi WB}, \quad (2.3)$$

however looking into the tree-level dictionary [44] we can see that these operators can only come from one-loop processes, if we assume that the UV-Lagrangian contains terms only up to dimension 4, and restrict ourselves to UV models containing only scalars and/or fermions. These operators can of course come at tree level, if we already have operators with dimension greater than 4, or include vector fields in the discussion.

What we can do to disentangle the tree and loop level contributions is to split the coefficients into their tree and loop level parts as follows, $C = C^{[0]} + \frac{1}{16\pi^2} C^{[1]} \simeq C^{[0]} + 0.6 \times 10^{-2} C^{[1]}$. This re-scales all coefficients so that we can easily compare between contributions of different operators. Apart from the tree-loop split, for the case of the three Wilson coefficients mentioned above, we can do another re-scaling, $C^{\phi B} \rightarrow g'^2 \hat{C}^{\phi B}$, $C^{\phi W} \rightarrow g^2 \hat{C}^{\phi W}$, $C^{\phi WB} \rightarrow g'g \hat{C}^{\phi WB}$. We can immediately see that in both expressions the operators $C^{(e,u,d)(B,W)}$, C^W , are way too small since they occur at one-loop. We can

also observe that the combination of the three Wcs $C_{1221}^{\ell\ell}$, $C_{11,22}^{\phi\ell(3)}$ constitute the corrections of SMEFT to the Fermi constant, which is known to high accuracy. The corrections of the Fermi constant in the SMEFT read [47, 48],

$$G_F^{\text{SMEFT}} = G_F + \delta G_F, \quad (2.4)$$

where $G_F = 1.1663787(6) \times 10^{-5} \text{ GeV}^{-2}$ and $\delta G_F = -\frac{1}{\sqrt{2}} \left(C_{1221}^{\ell\ell} - C_{11}^{\phi\ell(3)} - C_{22}^{\phi\ell(3)} \right)$.

So, we re-write the formulas with the re-scaled contributions, setting the renormalization scale to $\mu = \Lambda = 1 \text{ TeV}$ and the correction above so as to compare the coefficients again,

$$\begin{aligned} \delta R_{h \rightarrow Z\gamma} &\simeq -0.25 \delta G_F + 0.12 \left(C^{[0]\phi\Box} - C^{[0]\phi D} \right) \\ &\quad + 0.01 \hat{C}^{[1]\phi B} - 0.04 \hat{C}^{[1]\phi W} + 0.01 \hat{C}^{[1]\phi WB} \\ &\quad - 0.01 \left(C_{33}^{[0]d\phi} - C_{33}^{[0]u\phi} \right) + \dots, \end{aligned} \quad (2.5)$$

$$\begin{aligned} \delta R_{h \rightarrow \gamma\gamma} &\simeq -0.25 \delta G_F + 0.12 \left(C^{[0]\phi\Box} - 2C^{[0]\phi D} \right) \\ &\quad - 0.03 \hat{C}^{[1]\phi B} - 0.04 \hat{C}^{[1]\phi W} + 0.03 \hat{C}^{[1]\phi WB} \\ &\quad - 0.01 \left(C_{22}^{[0]e\phi} + 4C_{33}^{[0]e\phi} + 5C_{22}^{[0]u\phi} + 2C_{33}^{[0]d\phi} - 3C_{33}^{[0]u\phi} \right) + \dots. \end{aligned} \quad (2.6)$$

Disentangling the formulas in such a way provides us with more insight on the values of the couplings that we can expect in the UV. With this procedure we have also narrowed down a multitude of contributing operators to just a handful of them making the study of these two observables easier.

A few remarks are in order.

- The largest contributions to $\delta R_{h \rightarrow \gamma\gamma}$ no longer comes from the operator $C^{\phi B}$ even though initially that was the case. The most dominant Wcs are $C_{1221}^{\ell\ell}$, $C_{11}^{\phi\ell(3)}$, $C_{22}^{\phi\ell(3)}$, while next in line are the Wcs $C^{\phi D}$ and $C^{\phi\Box}$. Incidentally these five operators contribute maximally to $\delta R_{h \rightarrow Z\gamma}$ as well. Consequently, the model in question must not generate $C_{1221}^{\ell\ell}$ solely, this would give a high correction to the Fermi constant which is excluded, unless we tune down its couplings to minuscule values.
- We also note that the correction to the Fermi constant has to be negligible of the order of 10^{-6} . Wilson coefficients $C^{\phi\Box}$ and $C^{\phi D}$ could cancel each other out if $C^{\phi\Box} = 2C^{\phi D}$ and that could boost $h \rightarrow Z\gamma$, or they are not generated at tree level and are suppressed by a loop factor. However in the case of a cancellation that would leave only $C^{\phi D}$ which is heavily constrained by the T -parameter as we will also see below.
- What values of Wcs would it take to boost $h \rightarrow Z\gamma$ while simultaneously these Wcs would destructively contribute in $h \rightarrow \gamma\gamma$? Ideally we would like to avoid generating the dominant tree level Wcs mentioned above because they equally contribute to both observables and there is no apparent way to cancel each other out. Our main goal is to restore the dominance of $C^{\phi(B,W,WB)}$ Wcs.
- For both signal strengths their expressions are almost identical with the only difference being the Wc $C_{pp}^{e\phi}$ which contributes only to $\delta R_{h \rightarrow \gamma\gamma}$, however operators of such kind arising from the tree level are usually suppressed by the Yukawa coupling of the corresponding fermion and are thus suppressed for the most part. For this reason we will keep from now on only contributions from the third generation of quarks.
- In the expressions in eq.(2.1) and eq.(2.2) for the signal strengths all Wcs are considered at the renormalization scale μ , $C(\mu)$. Since we have split the operators in the tree and loop counterparts

the RG mixing of loop level operators constitutes a two loop effect and is neglected. Since we have set $\mu = \Lambda = 1$ TeV, all Wcs are from now on considered at $C(\mu) = C(\Lambda)$.

We can construct a chi-square function to explore further the correlations and the required numerical values that these three coefficients need to take to accommodate an excess in one over the other observable. The observables that we choose to add are the decay and production modes of the Higgs boson which can fairly constrain all Wcs in our study. Apart from the observables above we add the oblique parameters S and T , because they highly constrain $C^{\phi WB}$ and $C^{\phi D}$ respectively. In the $\{G_F, M_W, M_Z\}$ scheme, these two expressions read,

$$\Delta S = \frac{2\pi}{G_F^2 M_W \sqrt{M_Z^2 - M_W^2}} \frac{C^{\phi WB}}{\Lambda^2}, \quad (2.7)$$

$$\Delta T = \frac{\pi}{4G_F^2} \frac{M_Z^2}{M_W^2(M_Z^2 - M_W^2)} \frac{C^{\phi D}}{\Lambda^2} \quad (2.8)$$

Substituting the relevant values and setting $\Lambda = 1$ TeV, we get the semi-numerical expression shown below,

$$\Delta S = 0.0199 \hat{C}_{\phi WB}, \quad (2.9)$$

$$\Delta T = -4.0083 C^{\phi D}. \quad (2.10)$$

The experimental values of decay and production channels that we are using to construct the χ^2 function are shown in the table below. For S and T parameters we have the following two experimental values and corresponding uncertainties, $S_{\text{exp}} = -0.02 \pm 0.07$ and $T_{\text{exp}} = 0.04 \pm 0.06$ [49].

Decay	Experiment	Production	Experiment
$\mu_{h \rightarrow \gamma\gamma}$	1.10 ± 0.07	μ_{ggF}	0.97 ± 0.08
$\mu_{h \rightarrow Z\gamma}$	2.20 ± 0.70 [15]	μ_{VBF}	0.80 ± 0.12
$\mu_{h \rightarrow ZZ^*}$	1.02 ± 0.08	μ_{Wh}	1.44 ± 0.26
$\mu_{h \rightarrow WW^*}$	1.00 ± 0.08	μ_{Zh}	1.29 ± 0.25
$\mu_{h \rightarrow \mu^+ \mu^-}$	1.21 ± 0.35	μ_{tth}	0.94 ± 0.20
$\mu_{h \rightarrow \tau^+ \tau^-}$	0.91 ± 0.09		
$\mu_{h \rightarrow b\bar{b}}$	0.99 ± 0.12		

Table 1: Numerical values used to construct the χ^2 function to be minimized. The decay channel values were taken from [49], except for the $h \rightarrow Z\gamma$ decay. The production channel experimental values were taken from CMS [13].

We define the χ^2 , below,

$$\chi^2 = (O^{\text{SMEFT}} - O^{\text{exp}})^T (\sigma^2)^{-1} (O^{\text{SMEFT}} - O^{\text{exp}}), \quad (2.11)$$

where O^{exp} is the column vector that contains the central values of the experimental measurements of the corresponding signal strengths of Table 1, while in this case σ^2 is a $N_{\text{obs}} \times N_{\text{obs}}$ diagonal matrix containing the relevant uncertainties, where we have neglected theory uncertainties and assumed that all measurements are uncorrelated. The quantity O^{SMEFT} can be decomposed into two pieces, a purely SM piece, O^{SM} and a purely BSM piece, O^{BSM} . Since the SM piece is a pure number we subtract it from the experimental values and we define $O^\delta = O^{\text{SM}} - O^{\text{exp}}$. We use Singular Value Decomposition (SVD) technique as described in [50] to solve this least squares problem and we cross-check the results by also minimizing the chi-square function. The set of Wcs we consider here are

$$\{C^{\phi B}, C^{\phi W}, C^{\phi WB}, C^{\phi \square}, C^{\phi D}, C_{33}^{u\phi}, C_{33}^{d\phi}\}, \quad (2.12)$$

where we neglect the Wcs that affect corrections to the Fermi constant.

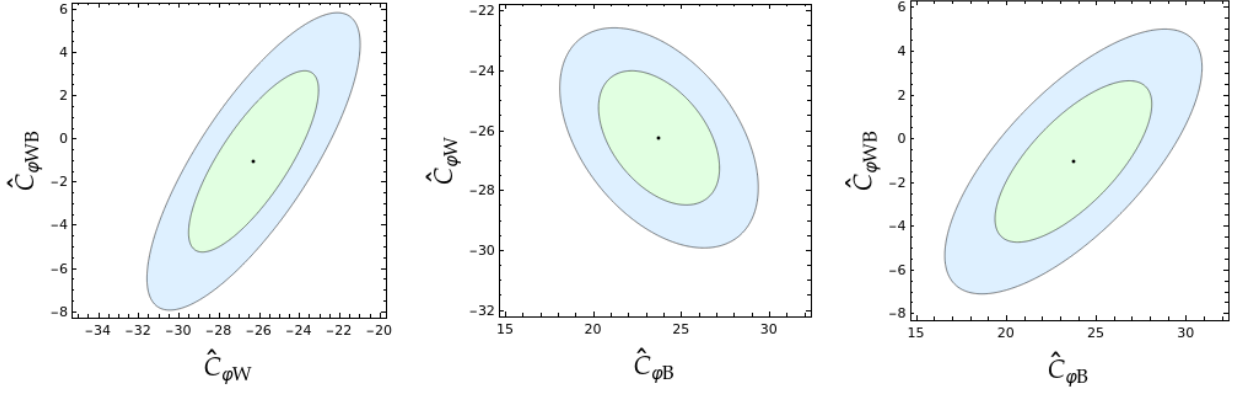


Fig. 1: Error ellipses drawn by setting each respective coefficient to its best-fit value while varying the other two. Green and light blue contours represent, 1σ and 2σ respectively.

The best-fit values for the Wilson coefficients that we obtain, for $\Lambda = 1$ TeV are,

$$\hat{C}^{\phi B} = 23.75 \pm 3.03 , \quad (2.13)$$

$$\hat{C}^{\phi W} = -26.26 \pm 2.68 , \quad (2.14)$$

$$\hat{C}^{\phi WB} = -1.07 \pm 3.63 , \quad (2.15)$$

$$C^{\phi \square} = -0.18 \pm 0.40 , \quad (2.16)$$

$$C^{\phi D} = 0.01 \pm 0.01 , \quad (2.17)$$

$$C_{33}^{u\phi} = -0.83 \pm 1.21 , \quad (2.18)$$

$$C_{33}^{d\phi} = 0.001 \pm 0.03 . \quad (2.19)$$

The correlation matrix for these coefficients, is,

Wcs	$C^{\phi B}$	$C^{\phi W}$	$C^{\phi WB}$	$C^{\phi \square}$	$C^{\phi D}$	$C_{33}^{u\phi}$	$C_{33}^{d\phi}$
$C^{\phi B}$	1.	0.268	0.633	0.073	-0.013	0.192	0.032
$C^{\phi W}$		1.	0.613	0.539	-0.007	0.335	0.205
$C^{\phi WB}$			1.	0.003	0	0.001	0.001
$C^{\phi \square}$				1.	0.03	0.33	0.374
$C^{\phi D}$					1.	0.006	0.007
$C_{33}^{u\phi}$						1.	0.157
$C_{33}^{d\phi}$							1.

From the covariance matrix of the coefficients we can also draw the error ellipses, as shown in Figure 1. In each of the plots we have set each respective coefficient that is not drawn to its best-fit values and have drawn error ellipses of the other two. So, for example, in the first plot we have set every coefficient but $C_{\phi W}$ and $C_{\phi WB}$ to its best-fit value and have plotted the error ellipses of the other two.

Let us now lay down the requirements that UV models would need to have in order to be a viable option to study further:

1. The most important relation that needs to hold is that $C^{\phi B}$ and $C^{\phi W}$ need to come with a definite sign difference. This firstly means that the UV model has to generate both. This alone could accommodate for an excess in $h \rightarrow Z\gamma$ if we don't generate any other Wc that affects the two observables equally.
2. We also notice that if $C^{\phi WB}$ is generated it would need to be small, even accounting for uncertainties because of the direct relation to the S -parameter.

3. Some models could generate also a pair of $C^{\phi\Box}$ and $C^{\phi D}$, if they are generated together at tree level they are proportional to each other. From the fit above we see that including uncertainties it could be possible to accommodate this possibility.

3 Single field UV models

The following sections examine the single field extensions of the tree level dictionary [44, 51] as well as some potential two field cases. The list below is not exhaustive but it tries to filter out favorable models for this case. To get all the expressions of the relevant loop generated operators we use the package SOLD [41], which contains all information on Wcs exclusively generated at one-loop order form scalar and vector like fermion extensions. We refrain from including or discussing massive vector bosons for a couple of reasons. First, no automated package exists up to date that could give us immediately Wcs and facilitate our study. Second and most important, we would need to account for the gauge boson mass, which would require the inclusion of a spontaneous symmetry breaking mechanism able to explain the origin of the mass. Additionally, if we consider vector bosons the Wcs that are of interest, namely $C^{\phi(B,W,WB)}$, are generated at tree level and are either coming from already non renormalizable interactions of dimension greater than four, or in some cases even if these operators are coming from interactions of dimension less or equal to four there is never a sign difference between Wcs $C^{\phi B}$ and $C^{\phi W}$ [44]. The inclusion of vector boson extensions is outside the scope of this study. Additionally, barring vector boson extensions, CP-violating operators come from interactions of already non-renormalizable operators in the models that we investigate, we restrict ourselves to interactions of the original Lagrangian up to mass dimension four.

3.1 The case for BSM scalars

To examine some viable scenarios we list in the table below all scalar fields that serve as extensions of the SM, that also have a linear coupling with the SM particle content. We also list the tree level operators that they generate as well as the subset of loop level operators that are interesting for our case study. We omit colored fields since these generate the operator $\mathcal{O}^{\phi G}$, which largely contributes to the production rate of ggF and this production channel is a very well measured quantity, so we want to avoid this bound.

Fields	Irrep	Tree level operators	Loop level operators
\mathcal{S}	$(1, 1)_0$	$\mathcal{O}^{\phi\Box}$	$\mathcal{O}_{\phi B}, \mathcal{O}_{\phi W}, \mathcal{O}_{\phi WB}$
\mathcal{S}_1	$(1, 1)_1$	$\mathcal{O}^{\ell\ell}$	$\mathcal{O}_{\phi B}$
\mathcal{S}_2	$(1, 1)_2$	\mathcal{O}^{ee}	$\mathcal{O}_{\phi B}$
φ	$(1, 2)_{1/2}$	$\mathcal{O}^{(e,u,d)\phi}$	$\mathcal{O}_{\phi B}, \mathcal{O}_{\phi W}, \mathcal{O}_{\phi WB}$
Ξ	$(1, 3)_0$	$\mathcal{O}^{\phi D}, \mathcal{O}^{\phi\Box}, \mathcal{O}^{(e,u,d)\phi}$	$\mathcal{O}_{\phi B}, \mathcal{O}_{\phi W}$
Ξ_1	$(1, 3)_1$	$\mathcal{O}^{\phi D}, \mathcal{O}^{\phi\Box}, \mathcal{O}^{(e,u,d)\phi}$	$\mathcal{O}_{\phi B}, \mathcal{O}_{\phi W}, \mathcal{O}_{\phi WB}$
Θ_1	$(1, 4)_{1/2}$	\mathcal{O}^{ϕ}	$\mathcal{O}_{\phi B}, \mathcal{O}_{\phi W}, \mathcal{O}_{\phi WB}$
Θ_3	$(1, 4)_{3/2}$	\mathcal{O}^{ϕ}	$\mathcal{O}_{\phi B}, \mathcal{O}_{\phi W}, \mathcal{O}_{\phi WB}$

Table 2: Tree and relevant loop level operators generated by new scalar field extensions of the SM related to these two signal strengths.

- Field \mathcal{S} , a neutral scalar generates all the necessary operators, the expressions are found below. Where we present as a subscript the relevant schematic interaction that this coupling is coming from.

$$C^{\phi\Box} = -\frac{(\kappa_{\mathcal{S}\phi^2})^2}{2M_{\mathcal{S}}^4}, \quad \hat{C}^{\phi WB} = 2\hat{C}^{\phi B} = 2\hat{C}^{\phi W} = \frac{(\kappa_{\mathcal{S}\phi^2})^2}{6M_{\mathcal{S}}^4}. \quad (3.1)$$

This set of Wcs would be impossible to explain a possible deviation because we have a universal contribution to $C^{\phi\Box}$ and there is also no way to get a sign difference because $C^{\phi B} = C^{\phi W}$.

- Fields $\mathcal{S}_{1,2}$, charged singlets do no generate the required set of operators necessary for our purposes. Additionally, \mathcal{S}_1 , gives $C_{\ell\ell}$ which would potentially contribute strongly to Fermi constant. The Wcs are shown below for completeness,

$$\mathcal{S}_1 : \quad (C^{\ell\ell})_{ijkl} = \frac{(y_{\mathcal{S}_1\ell\ell^c})_{jl}^* (y_{\mathcal{S}_1\ell\ell^c})_{ik}}{M_{\mathcal{S}_1}^2}, \quad \hat{C}^{\phi B} = -\frac{\lambda_{\mathcal{S}_1^2\phi^2}}{12M_{\mathcal{S}_1}^2}, \quad (3.2)$$

$$\mathcal{S}_2 : \quad (C^{ee})_{ijkl} = \frac{(y_{\mathcal{S}_2ee^c})_{lj}^* (y_{\mathcal{S}_2ee^c})_{ki}}{2M_{\mathcal{S}_2}^2}, \quad \hat{C}^{\phi B} = -\frac{\lambda_{\mathcal{S}_2^2\phi^2}}{3M_{\mathcal{S}_2}^2}. \quad (3.3)$$

So, we exclude these two single fields as well.

- Next is the 2HDM, where a recent work [52] also explores the matching of this model and fits to relevant Higgs observables. Field φ generates the correct set given below,

$$\hat{C}^{\phi B} = \hat{C}^{\phi W} = -\frac{3\sqrt{2}\kappa_{\varphi^2\phi^2} + 2\lambda_{\varphi^2\phi^2}}{96M_{\varphi}^2}, \quad \hat{C}^{\phi WB} = -\frac{\sqrt{2}\kappa_{\varphi^2\phi^2} - 2\lambda_{\varphi^2\phi^2}}{48M_{\varphi}^2}, \quad (3.4)$$

$$(C^{e\phi})_{ij} = \frac{\lambda_{\varphi\phi^3}(y_{e\varphi})_{ji}^*}{M_{\varphi}^2}, \quad (C^{d\phi})_{ij} = \frac{\lambda_{\varphi\phi^3}(y_{d\varphi})_{ji}^*}{M_{\varphi}^2}, \quad (C^{u\phi})_{ij} = -\frac{\lambda_{\varphi\phi^3}^*(y_{u\varphi})_{ji}}{M_{\varphi}^2}. \quad (3.5)$$

Again here the Higgs-gauge boson operators are generated but the two most important ones are equal. For this reason we exclude this model.

- Next we consider electroweak triplets. First Ξ generates the following operators,

$$C^{\phi\Box} = -\frac{1}{4}C^{\phi D} = \frac{\kappa_{\Xi\phi^2}^2}{2M_{\Xi}^4}, \quad (3.6)$$

$$C^{\phi B} = \frac{\kappa_{\Xi\phi^2}^2}{16M_{\Xi}^4}, \quad C^{\phi W} = -\frac{1}{4}C^{\phi B} + \frac{\lambda_{\Xi^2\phi^2}}{6\sqrt{6}M_{\Xi}^2}, \quad (3.7)$$

$$(C^{e\phi})_{ij} = \frac{\kappa_{\Xi\phi^2}^2(y_e)_{ji}^*}{M_{\Xi}^4}, \quad (C^{d\phi})_{ij} = \frac{\kappa_{\Xi\phi^2}^2(y_d)_{ji}^*}{M_{\Xi}^4}, \quad (C^{u\phi})_{ij} = -\frac{\kappa_{\Xi\phi^2}^2(y_u)_{ji}^*}{M_{\Xi}^4}, \quad (3.8)$$

where $y_{(e,u,d)}$ are the usual Yukawa coupling of the SM. Although the model looks promising since it generates all Wc required these Wcs are heavily correlated to each other, we can write down the following relations, $C^{\phi\Box} = -C^{\phi D}/4 = 8C^{\phi B}$, $(C^{(e,d)\phi})_{ij} = 2(y_{(e,d)})_{ji}^* C^{\phi\Box}$ and $(C^{u\phi})_{ij} = -2(y_u)_{ji}^* C^{\phi\Box}$. The most stringent constraint for this model comes from the T -parameter which is proportional to $C^{\phi D}$ and forces us to a small value for this Wc which is related to $C^{\phi B}$ which we want it to be large. We can write down the following observables to for a more clear picture, where we only keep the top Yukawa coupling and neglect the other contributions since they are too small,

$$\Delta T = -8.016 \frac{\kappa_{\Xi\phi^2}^2}{M_{\Xi}^4}, \quad (3.9)$$

$$\delta R_{h \rightarrow \gamma\gamma} = 0.508 \frac{\kappa_{\Xi\phi^2}^2}{M_{\Xi}^4} - 0.0025 \frac{\lambda_{\Xi^2\phi^2}}{M_{\Xi}^2}, \quad (3.10)$$

$$\delta R_{h \rightarrow Z\gamma} = 0.2912 \frac{\kappa_{\Xi\phi^2}^2}{M_{\Xi}^4} - 0.0026 \frac{\lambda_{\Xi^2\phi^2}}{M_{\Xi}^2}. \quad (3.11)$$

In order to satisfy the bound for the T -parameter, which in our case needs to be negative and by taking the lower bound of the experimental value at $T_{\text{exp}} \geq -0.02$, we get the bound for

the coupling to mass ratio $\kappa_{\Xi\phi^2}^2/M_{\Xi}^4 \geq 25 \times 10^{-4}$, substituting these values into the observables above we get,

$$\delta R_{h \rightarrow \gamma\gamma} = 0.0013 - 0.0025 \frac{\lambda_{\Xi^2\phi^2}}{M_{\Xi}^2}, \quad (3.12)$$

$$\delta R_{h \rightarrow Z\gamma} = 0.0007 - 0.0026 \frac{\lambda_{\Xi^2\phi^2}}{M_{\Xi}^2}. \quad (3.13)$$

These contributions are way too small and we are left with a universal contribution of the quartic coupling of the triplet with the Higgs which cannot serve our purpose of splitting apart the two observables. We rule out this model as well.

- The next triplet, Ξ_1 is charged and the corresponding Wcs are,

$$C^{\phi\Box} = \frac{1}{2} C^{\phi D} = \frac{2|\kappa_{\Xi_1\phi^2}|^2}{M_{\Xi}^4}, \quad C^{\phi WB} = -\frac{5|\kappa_{\Xi_1\phi^2}|^2}{12M_{\Xi}^4} - \frac{\lambda'_{\Xi_1^2\phi^2}}{6\sqrt{3}M_{\Xi}^2}, \quad (3.14)$$

$$C^{\phi B} = -\frac{|\kappa_{\Xi_1\phi^2}|^2}{4M_{\Xi}^4} + \frac{\lambda_{\Xi_1^2\phi^2}}{4\sqrt{6}M_{\Xi}^2}, \quad C^{\phi W} = -\frac{|\kappa_{\Xi_1\phi^2}|^2}{12M_{\Xi}^4} + \frac{\lambda_{\Xi_1^2\phi^2}}{6\sqrt{6}M_{\Xi}^2}, \quad (3.15)$$

$$\left(C^{e\phi}\right)_{ij} = \frac{2|\kappa_{\Xi_1\phi^2}|^2 (y_e)_{ji}^*, \quad \left(C^{d\phi}\right)_{ij} = \frac{2|\kappa_{\Xi_1\phi^2}|^2 (y_d)_{ji}^*, \quad \left(C^{u\phi}\right)_{ij} = -\frac{2|\kappa_{\Xi_1\phi^2}|^2 (y_u)_{ji}^*}{M_{\Xi}^4}. \quad (3.16)$$

In this case again the operators are directly related to each other, we can rewrite $C^{\phi W}$ as follows, $C^{\phi W} = C^{\phi B}/3 + \frac{\lambda_{\Xi_1^2\phi^2}}{12\sqrt{6}M_{\Xi}^2}$, this relation shows that we cannot easily change the sign of these two operators since they are directly related. Also strong constraints for the coupling $\kappa_{\Xi_1\phi^2}$ come from the T -parameter. But let's write everything down first,

$$\Delta T = 16.033 \frac{|\kappa_{\Xi_1\phi^2}|^2}{M_{\Xi}^4}, \quad (3.17)$$

$$\Delta S = -0.008 \frac{|\kappa_{\Xi_1\phi^2}|^2}{M_{\Xi}^4} - 0.0019 \frac{\lambda'_{\Xi_1^2\phi^2}}{M_{\Xi}^2}, \quad (3.18)$$

$$\delta R_{h \rightarrow \gamma\gamma} = 0.720 \frac{|\kappa_{\Xi_1\phi^2}|^2}{M_{\Xi}^4} - \frac{0.0067\lambda_{\Xi_1^2\phi^2} + 0.0033\lambda'_{\Xi_1^2\phi^2}}{M_{\Xi}^2}, \quad (3.19)$$

$$\delta R_{h \rightarrow Z\gamma} = 0.244 \frac{|\kappa_{\Xi_1\phi^2}|^2}{M_{\Xi}^4} - \frac{0.0015\lambda_{\Xi_1^2\phi^2} + 0.0011\lambda'_{\Xi_1^2\phi^2}}{M_{\Xi}^2}. \quad (3.20)$$

Setting the T-parameter to be of the order of $T \sim 10^{-2}$, we can get a bound for the ratio $|\kappa_{\Xi_1\phi^2}|^2/M_{\Xi}^4 \sim 0.6 \times 10^{-3}$ and we rewrite the rest,

$$\Delta S \simeq -0.19 \times 10^{-2} \frac{\lambda'_{\Xi_1^2\phi^2}}{M_{\Xi}^2}, \quad (3.21)$$

$$\delta R_{h \rightarrow \gamma\gamma} \simeq -10^{-2} \frac{0.67\lambda_{\Xi_1^2\phi^2} + 0.33\lambda'_{\Xi_1^2\phi^2}}{M_{\Xi}^2}, \quad (3.22)$$

$$\delta R_{h \rightarrow Z\gamma} \simeq -10^{-2} \frac{0.15\lambda_{\Xi_1^2\phi^2} + 0.11\lambda'_{\Xi_1^2\phi^2}}{M_{\Xi}^2}. \quad (3.23)$$

From these relation we can see that the two signal strengths cannot be separated. This model is also explored in ref [20]. The same conclusion is reached and can be seen in their Figure 6 panel (c), where the difference $\delta R_{h \rightarrow \gamma\gamma} - \delta R_{h \rightarrow Z\gamma}$ is plotted.

- Moving on the last two scalar fields we have a charged field labeled Θ_1 in the 4-representation of $SU(2)$. This generates the operators below,

$$C^{\phi B} = \frac{\lambda_{\Theta_1^2 \phi^2}}{16\sqrt{6} M_{\Theta_1}^2}, \quad C^{\phi W} = 4 C^{\phi B}, \quad C^{\phi WB} = -\frac{\lambda'_{\Theta_1^2 \phi^2}}{12\sqrt{3} M_{\Theta_1}^2}. \quad (3.24)$$

It is evident that we cannot under any circumstance get opposite signs for $C^{\phi B}$ and $C^{\phi W}$.

- The same situation stands for the other charged field labeled, Θ_3 , but we list here the generated operators for completeness.

$$C^{\phi B} = \frac{9 \lambda_{\Theta_3^2 \phi^2}}{16\sqrt{6} M_{\Theta_3}^2}, \quad C^{\phi W} = \frac{8}{27} C^{\phi B}, \quad C^{\phi WB} = -\frac{\lambda'_{\Theta_3^2 \phi^2}}{4\sqrt{3} M_{\Theta_3}^2}. \quad (3.25)$$

3.2 The case for vector-like fermions

Barring chiral fermions, where constraints from multiple Higgs observables have ruled out this scenario [19], we can extend the fermion content of the SM by the fields shown in the table below.

Fields	Irrep	Tree level operators	Loop level operators
N	$(1, 1)_0$	$\mathcal{O}_5, \mathcal{O}_{\phi\ell}^{(1,3)}$	$\mathcal{O}_{\phi B}, \mathcal{O}_{\phi W}, \mathcal{O}_{\phi WB}$
E	$(1, 1)_{-1}$	$\mathcal{O}_{e\phi}, \mathcal{O}_{\phi\ell}^{(1,3)}$	$\mathcal{O}_{\phi B}, \mathcal{O}_{\phi W}, \mathcal{O}_{\phi WB}$
Δ_1	$(1, 2)_{-1/2}$	$\mathcal{O}_{e\phi}, \mathcal{O}_{\phi e}$	$\mathcal{O}_{\phi B}, \mathcal{O}_{\phi WB}$
Δ_3	$(1, 2)_{-3/2}$	$\mathcal{O}_{e\phi}, \mathcal{O}_{\phi e}$	$\mathcal{O}_{\phi B}, \mathcal{O}_{\phi WB}$
Σ	$(1, 3)_0$	$\mathcal{O}_5, \mathcal{O}_{e\phi}, \mathcal{O}_{\phi\ell}^{(1,3)}$	$\mathcal{O}_{\phi B}, \mathcal{O}_{\phi W}, \mathcal{O}_{\phi WB}$
Σ_1	$(1, 3)_{-1}$	$\mathcal{O}_{e\phi}, \mathcal{O}_{\phi\ell}^{(1,3)}$	$\mathcal{O}_{\phi B}, \mathcal{O}_{\phi W}, \mathcal{O}_{\phi WB}$

Table 3: Tree level operators generated by new vector-like fermions.

The case here is clearer than the scalars because we will always need two fermions to make up interactions with the Higgs and this saturates the dimension of the corresponding operator fast. For completeness we list the generated Wcs for each fermion below although none of them can accommodate to the splitting of the observables because their Wcs are proportional and the dominant ones i.e. $C^{\phi B}$ and $C^{\phi W}$ come also with the same sign:

$$N : \quad C^{\phi B} = C^{\phi W} = \frac{1}{2} C^{\phi WB} = \frac{|\lambda_{N\phi\ell}|^2}{24M_N^2}, \quad (3.26)$$

$$E : \quad C^{\phi B} = 3 C^{\phi W} = -\frac{3}{4} C^{\phi WB} = \frac{|\lambda_{E\phi\ell}|^2}{8M_E^2}, \quad (3.27)$$

$$\Delta_1 : \quad C^{\phi B} = -3 C^{\phi WB} = \frac{|\lambda_{\Delta_1\phi e}|^2}{4M_{\Delta_1}^2}, \quad C^{\phi W} = 0, \quad (3.28)$$

$$\Delta_3 : \quad C^{\phi B} = 5 C^{\phi WB} = \frac{5 |\lambda_{\Delta_3\phi e}|^2}{12M_{\Delta_3}^2}, \quad C^{\phi W} = 0, \quad (3.29)$$

$$\Sigma : \quad C^{\phi B} = \frac{3}{7} C^{\phi W} = -\frac{1}{2} C^{\phi WB} = \frac{|\lambda_{\Sigma\phi\ell}|^2}{32M_{\Sigma}^2}, \quad (3.30)$$

$$\Sigma_1 : \quad C^{\phi B} = \frac{9}{7} C^{\phi W} = \frac{9}{8} C^{\phi WB} = \frac{3 |\lambda_{\Sigma_1\phi\ell}|^2}{32M_{\Sigma_1}^2}. \quad (3.31)$$

Summing up, we presented all relevant Wcs, both tree and loop level, of single field extensions, of scalars and fermions, that primarily affect the signal strengths $\delta R_{h \rightarrow \gamma\gamma}$ and $\delta R_{h \rightarrow Z\gamma}$. We have found

that no single field can accommodate a potential excess in one observable over the other. We must also mention that we can extend this list of fields with particles that do not have any linear coupling with the SM and leave the hypercharge as a general parameter that we can fit to find the suitable value. However, these contributions come from the quartic interactions with the Higgs and can give no value that could fit into the single field scheme that we discussed above. They can come in handy when we are discussing two field extensions below.

As a general remark we note that the value of the W_c that we are trying to reach is way above what is being produced here in the one field cases. The coefficients that multiply the coupling to mass ratio range from 10^{-1} all the way to 10^{-3} , ideally we would like to raise the values by one or two orders of magnitude to meet the requirements presented in the SMEFT analysis. The solution to this issue is difficult because the mass of the heavy field cannot go much lower due to EFT convergence, and the coupling cannot go higher than 4π due to perturbativity. In reality, our hands are bind to resort to options with more fields, hoping that these contributions might pile up.

4 Two-field models

In the two field case scenarios we have a plethora of combinations to work with. We can combine scalars (fermions) with scalars (fermions) and scalars with fermions and analyze each model that shows some promising characteristics on W_c s. In order to tackle the number of models that arise from these combinations we can rely on the single field results and add on top of that new scalar and/or fermion fields that could amend the situation.

In disentangling the two-field models we will try and categorize the interactions and their corresponding W_c s taking hints from their matching of universal coefficients and how the operators $C^{\phi(B,W,WB)}$ are actually generated. We will develop our rationale in terms of covariant traces/diagrams [24] stemming from the UOLEA [26] and its corresponding byproducts [25, 27, 29–34, 42]. In order to generate the operators $C^{\phi(B,W,WB)}$, we need the functional traces to contain $G'_{\mu\nu} G'_{\mu\nu}$, where $G'_{\mu\nu} = -igG_{\mu\nu}$ where g is the corresponding coupling of the field strength tensor $G_{\mu\nu}$, which directly relates to the gauge group representations of the field. If the fields have representations under several groups a summation over the different strength tensors is understood. There are two such traces in the heavy-only UOLEA and another two in the heavy-light UOLEA for scalar fields. The terms are shown below [42],

$$\tilde{f}_i^9 \text{tr} \{ U_{ii}^H G'_{i,\mu\nu} G'_{i,\mu\nu} \}, \quad \text{where,} \quad \tilde{f}_i^9 = -\frac{1}{12M_i^2}, \quad (4.1)$$

$$\tilde{f}_{ij}^{13} \text{tr} \{ U_{ij}^H U_{ji}^H G'_{i,\mu\nu} G'_{i,\mu\nu} \}, \quad \text{where,} \quad \tilde{f}_{ij}^{13} = \frac{2M_i^4 + 5M_i^2M_j^2 - M_j^4}{12M_i^2(\Delta_{ij}^2)^3} - \frac{M_i^2M_j^2}{2(\Delta_{ij}^2)^4} \log \left(\frac{M_i^2}{M_j^2} \right), \quad (4.2)$$

$$\tilde{f}_i^{13A} \text{tr} \{ U_{ii'}^{HL} U_{i'i}^{LH} G'_{i,\mu\nu} G'_{i,\mu\nu} \}, \quad \text{where,} \quad \tilde{f}_i^{13A} = \frac{1}{6M_i^4}, \quad (4.3)$$

$$\tilde{f}_i^{13B} \text{tr} \{ U_{i'i}^{LH} U_{ii'}^{HL} G'_{i',\mu\nu} G'_{i',\mu\nu} \}, \quad \text{where,} \quad \tilde{f}_i^{13B} = -\frac{1}{4M_i^4}. \quad (4.4)$$

A few definitions are in order. The coefficients are defined as $\tilde{f} = 16\pi^2 f$, the unprimed indices of the U -matrices denote the set of heavy fields, while the primed indices denote the set of light fields. We have also labeled the mass difference of the heavy fields as $\Delta_{ij}^2 = M_i^2 - M_j^2$ for brevity. The U -matrices are nothing more than differentiation of the Lagrangian with respect to the fields that the subscript indices denote, hence they contain both fields and couplings which in the end need to be traced throughout all available spaces of the fields (i.e. flavor, $SU(2)$, Lorentz etc.).

We can now categorize the interactions needed to produce our W_c s of interest through the terms above. For example in the first term (4.1) the mass dimension of U is $[U_{ii}^H] = 2$, which must contain

two Higgs fields to produce the desired operators, and it has been differentiated two times with respect to the heavy field, thus we can schematically write down the Lagrangian term as, $\Delta\mathcal{L} \sim X_i X_i H^\dagger H$. Following the same line of thought for the other two terms we can then write the correspondence below,

$$\tilde{f}_i^9 \text{tr} \{ U_{ii}^H G'_{i,\mu\nu} G'_{i,\mu\nu} \} \rightarrow \Delta\mathcal{L} \sim X_i X_i H^\dagger H, \quad (4.5)$$

$$\tilde{f}_{ij}^{13} \text{tr} \{ U_{ij}^H U_{ji}^H G'_{i,\mu\nu} G'_{i,\mu\nu} \} \rightarrow \Delta\mathcal{L} \sim X_i X_j H + \text{h.c.}, \quad (4.6)$$

$$\tilde{f}_i^{13A} \text{tr} \{ U_{ii'}^{HL} U_{i'i}^{LH} G'_{i,\mu\nu} G'_{i,\mu\nu} \} \text{ and } \tilde{f}_i^{13B} \text{tr} \{ U_{i'i}^{LH} U_{ii'}^{HL} G'_{i',\mu\nu} G'_{i',\mu\nu} \}, \rightarrow \Delta\mathcal{L} \sim X_i X_{i'} H + \text{h.c.} \quad (4.7)$$

We note that for (4.7), the only light scalar in the SM is the Higgs thus $X_{i'} = H$ and the interaction becomes $\Delta\mathcal{L} \sim X_i H^\dagger H$ and the only suitable fields have hypercharge $Y_i = 0$ and correspond to the neutral singlet S and the triplet Ξ , which were discussed above. We can then pair up these two fields with any other one to give us the desired operators. Next, eq.(4.5) conserves the hypercharge universally, that is this term is going to be present even if the value of the hypercharge is arbitrary. Lastly, eq.(4.6) is a linear coupling of the Higgs and the heavy fields so the hypercharge of the corresponding new fields have to obey the following rule, if we suppose that we leave Y_i free, the hypercharge of X_j is going to take the value $Y_j = Y_i + Y_H$ with $Y_H = 1/2$. Below we compose a table of available two-field models that could generate the operators $C^{\phi(B,W,WB)}$. We split the table depending on the field content, either we have two scalars labelled as (SS) , a scalar and a fermion labeled as (SF) or two fermions labeled as (FF) .

Model #	Field 1	Field 2	Tree Level
SS_{101Y_2}	$S_a \rightarrow (1, 1, 0)$	$S_b \rightarrow (1, 1, Y_2)$	$\mathcal{O}^{\phi\square}$
SS_{102Y_2}	$S_a \rightarrow (1, 1, 0)$	$S_b \rightarrow (1, 2, Y_2)$	$\mathcal{O}^{\phi\square}$
SS_{103Y_2}	$S_a \rightarrow (1, 1, 0)$	$S_b \rightarrow (1, 3, Y_2)$	$\mathcal{O}^{\phi\square}$
SS_{302Y_2}	$S_a \rightarrow (1, 3, 0)$	$S_b \rightarrow (1, 2, Y_2)$	$\mathcal{O}^{\phi\square}, \mathcal{O}^{\phi D}, \mathcal{O}^{(e,u,d)\phi}$
SS_{303Y_2}	$S_a \rightarrow (1, 3, 0)$	$S_b \rightarrow (1, 3, Y_2)$	$\mathcal{O}^{\phi\square}, \mathcal{O}^{\phi D}, \mathcal{O}^{(e,u,d)\phi}$
$SS_{1Y_12Y_2}$	$S_a \rightarrow (1, 1, Y_1)$	$S_b \rightarrow (1, 2, Y_1 + 1/2)$	-
$SS_{2Y_11Y_2}$	$S_a \rightarrow (1, 2, Y_1)$	$S_b \rightarrow (1, 1, Y_1 + 1/2)$	-
$SS_{2Y_13Y_2}$	$S_a \rightarrow (1, 2, Y_1)$	$S_b \rightarrow (1, 3, Y_1 + 1/2)$	-
$SS_{3Y_12Y_2}$	$S_a \rightarrow (1, 3, Y_1)$	$S_b \rightarrow (1, 2, Y_1 + 1/2)$	-
SF_{101Y_2}	$S_a \rightarrow (1, 1, 0)$	$F_b \rightarrow (1, 1, Y_2)$	$\mathcal{O}^{\phi\square}$
SF_{102Y_2}	$S_a \rightarrow (1, 1, 0)$	$F_b \rightarrow (1, 2, Y_2)$	$\mathcal{O}^{\phi\square}$
SF_{103Y_2}	$S_a \rightarrow (1, 1, 0)$	$F_b \rightarrow (1, 3, Y_2)$	$\mathcal{O}^{\phi\square}$
SF_{302Y_2}	$S_a \rightarrow (1, 3, 0)$	$F_b \rightarrow (1, 2, Y_2)$	$\mathcal{O}^{\phi\square}, \mathcal{O}^{\phi D}, \mathcal{O}^{(e,u,d)\phi}$
SF_{303Y_2}	$S_a \rightarrow (1, 3, 0)$	$F_b \rightarrow (1, 3, Y_2)$	$\mathcal{O}^{\phi\square}, \mathcal{O}^{\phi D}, \mathcal{O}^{(e,u,d)\phi}$
$FF_{1Y_12Y_2}$	$F_a \rightarrow (1, 1, Y_1)$	$F_b \rightarrow (1, 2, Y_1 + 1/2)$	-
$FF_{2Y_11Y_2}$	$F_a \rightarrow (1, 2, Y_1)$	$F_b \rightarrow (1, 1, Y_1 + 1/2)$	-
$FF_{2Y_13Y_2}$	$F_a \rightarrow (1, 2, Y_1)$	$F_b \rightarrow (1, 3, Y_1 + 1/2)$	-
$FF_{3Y_12Y_2}$	$F_a \rightarrow (1, 3, Y_1)$	$F_b \rightarrow (1, 2, Y_1 + 1/2)$	-

Table 4: Two field models that can generate $C^{\phi(B,W,WB)}$. We have established the following naming convention for the models. First two letters denote field content while the subscript denotes gauge quantum numbers under $SU(2) \times U(1)$. In total there are 18 candidate models.

Our strategy to determine the most we can get in the decay $h \rightarrow Z\gamma$ will be to construct a χ^2 with all observables mentioned in Table 1, excluding $h \rightarrow Z\gamma$ and leaving it as prediction of our model. We set bounds to the relevant couplings and masses and perform a constrained minimization of the χ^2

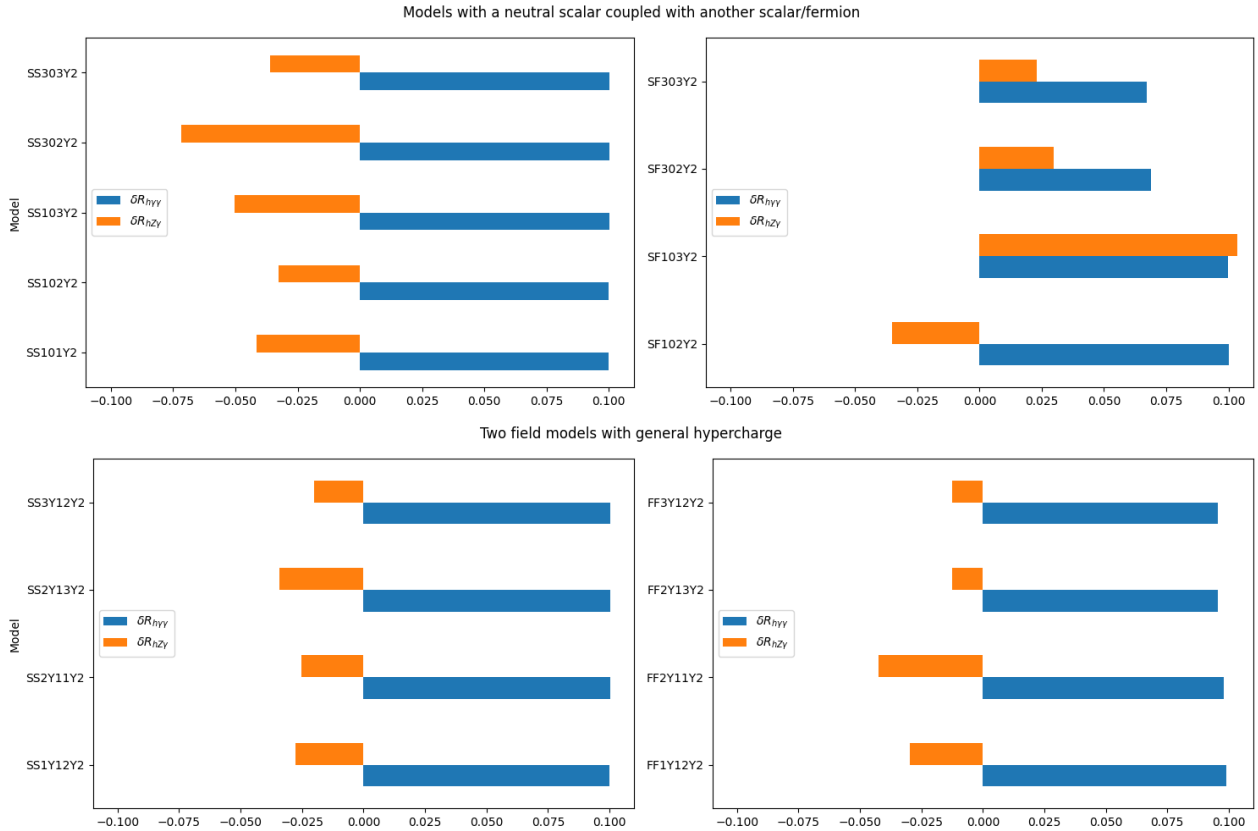


Fig. 2: The orange color represents the prediction of $h \rightarrow Z\gamma$ for each model and with orange is the values of $h \rightarrow \gamma\gamma$ obtained from the minimization of the couplings and masses (in the non-degenerate limit).

for each model. In the minimization we bound the couplings of each model to a range of $\lambda \sim [-2, 2]$ so as to account for perturbativity and for the masses we set the lowest values to be $M_{S(F)} \geq 0.7$ TeV to avoid issues with the EFT validity, since the lowest scale is the Higgs vev. In the models where the hypercharge relation obeys $Y_j = Y_i + 1/2$, the minimization with respect to the masses is more involved since there is also the degenerate mass limit that needs to be accounted for. In the non-degenerate case we restrict the mass difference to be greater than 0.1 TeV keeping of course the lowest bound of 0.7 TeV for both masses. We have also tested the degenerate mass limit, where in some cases we saw a slight improvement while in other cases we saw the gap between the two observables widen. Finally, we substitute the best fit values into $\delta R_{h \rightarrow Z\gamma}$ and get our prediction. The values of the corresponding Wcs are matched through the package SOLD [41] and we also perform the full matching of the model with MatchMakerEFT [40]. We provide as auxiliary files both the model files and the matching results that we obtained. More details can be found on Appendix B. In the figures above we present the results of the minimization procedure along with the prediction of $h \rightarrow Z\gamma$ of each respective model and the value of $h \rightarrow \gamma\gamma$ obtained by substituting the central values of the minimized couplings and masses. We observe that only one model predicts the value of $\delta R_{h \rightarrow Z\gamma}$ to be greater than that of $\delta R_{h \rightarrow \gamma\gamma}$. The only model capable to boost the one over the other observable, albeit with a negligible difference is SF_{103Y_2} , containing a neutral scalar singlet and a fermion triplet. The masses of the particles provided by the minimization subject to the constraints mentioned above are for the scalar $M_S = 1.62$ TeV and for the fermion $M_F = 0.7$ TeV, with a hypercharge $Y_2 = 0$. The exact values of the prediction is $\delta R_{h \rightarrow \gamma\gamma} = 0.099$ and $\delta R_{h \rightarrow Z\gamma} = 0.104$. Their difference is of the order $\sim 0.5\%$ with respect to the SM signal strength $\mu = 1$ and with the assumptions we have made on the models it can never reach the observed difference of the two signal strengths.

5 Conclusions

Following the first evidence of the Higgs boson decaying into a photon and a Z-boson by the ATLAS and CMS collaborations, we addressed the reported excess of $\sim 2\sigma$ [15]. We conducted a model-independent analysis in the SMEFT, incorporating various observables in both the decay and production channels of the Higgs boson. By performing a χ^2 -minimization, we found the best-fit values for each Wilson coefficient. This procedure reveals the most general relations among the Wcs to account for any discrepancy. Our main finding is that the Wilson coefficients $C^{\phi B}$ and $C^{\phi W}$ need to have opposite signs and have comparable magnitudes, while $C^{\phi WB}$ needs to be small since it's heavily constrained by the S -parameter.

Using our model-independent approach, we identified the necessary characteristics that UV models must possess to account for the excess in $h \rightarrow Z\gamma$. We considered all scalar and fermion single-field extensions of the SM that respect the SM gauge group but found that none could accommodate the data. Subsequently, we examined two-field models combining scalars and/or fermions. The candidate models were categorized based on their content and their universal loop-integral coefficient using the UOLEA.

We matched all UV models using automated packages and constructed a new χ^2 function, which we minimized with respect to model parameters. As shown in Figure 2, out of the 18 model families, only one specific model, which includes a neutral scalar singlet and a neutral fermion triplet, can boost $h \rightarrow Z\gamma$ while preserving the $h \rightarrow \gamma\gamma$ decay. However, this model still cannot fully accommodate the observed discrepancy in the data.

In summary, this study is valuable for providing the values and characteristics of Wcs capable of generating an enhancement in the decay channel $h \rightarrow Z\gamma$ over $h \rightarrow \gamma\gamma$. Moreover, the exploration of various two-field model families, surpassing the limitations of single-field models, provides insightful perspectives into potential UV physics behind this mild excess in $h \rightarrow Z\gamma$. If future data confirm this excess, our attention can pivot towards the investigation of alternative UV physics as the source of the discrepancy.

Acknowledgements

I would like to thank A. Dedes for his helpful suggestions on the manuscript and for his numerous discussions during the preparation of this work.

A Semi-numerical expressions of signal strengths

Here we provide the semi-numerical expressions of the signal strength corrections to the SM, in the decays and production channels of the Higgs boson, that we have used in this study. Apart from $\delta R_{h \rightarrow Z\gamma}$ and $\delta R_{h \rightarrow \gamma\gamma}$, which their one loop expressions are considered, found in [45, 46], all other formulas are taken to leading order from [52] and are computed in TeV^{-2} units. All expressions are given in the input scheme $\{G_F, M_W, M_Z\}$. We have split the signal strengths following the relation $\mu_i = 1 + \delta R_i$.

A.1 Decay channels

$$\delta R_{h \rightarrow b\bar{b}} = -5.050 C_{33}^{d\phi} + 0.121 (C^{\phi\Box} - \frac{1}{4} C^{\phi D}) + 0.0606 (C_{1221}^{\ell\ell} - C_{11}^{\phi\ell(3)} - C_{22}^{\phi\ell(3)}) , \quad (\text{A.1})$$

$$\delta R_{h \rightarrow WW^*} = -0.0895 C^{\phi W} + 0.121 (C^{\phi\Box} - \frac{1}{4} C^{\phi D}) + 0.0606 (C_{1221}^{\ell\ell} - C_{11}^{\phi\ell(3)} - C_{22}^{\phi\ell(3)}) , \quad (\text{A.2})$$

$$\delta R_{h \rightarrow \tau\bar{\tau}} = -11.88 C_{33}^{e\phi} + 0.121 (C^{\phi\Box} - \frac{1}{4} C^{\phi D}) + 0.0606 (C_{1221}^{\ell\ell} - C_{11}^{\phi\ell(3)} - C_{22}^{\phi\ell(3)}) , \quad (\text{A.3})$$

$$\begin{aligned} \delta R_{h \rightarrow ZZ^*} = & 0.296 (C^{\phi WB} - C^{\phi W}) - 0.197 C^{\phi B} + 0.119 C^{\phi\Box} + 0.005 C^{\phi D} + 0.181 C_{1221}^{\ell\ell} \\ & - 0.117 (C_{11}^{\phi\ell(3)} + C_{22}^{\phi\ell(3)}) , \end{aligned} \quad (\text{A.4})$$

$$\delta R_{h \rightarrow \mu\mu} = -199.79 C_{22}^{e\phi} + 0.121 (C^{\phi\Box} - \frac{1}{4} C^{\phi D}) , \quad (\text{A.5})$$

$$\begin{aligned} \delta R_{h \rightarrow Z\gamma} \simeq & 0.18 (C_{1221}^{\ell\ell} - C_{11}^{\phi\ell(3)} - C_{22}^{\phi\ell(3)}) + 0.12 (C^{\phi\Box} - C^{\phi D}) \\ & - 0.01 (C_{33}^{d\phi} - C_{33}^{u\phi}) + 0.02 (C_{33}^{\phi u} + C_{33}^{\phi q(1)} - C_{33}^{\phi q(3)}) \\ & + \left[14.99 - 0.35 \log \frac{\mu^2}{M_W^2} \right] C^{\phi B} - \left[14.88 - 0.15 \log \frac{\mu^2}{M_W^2} \right] C^{\phi W} + \left[9.44 - 0.26 \log \frac{\mu^2}{M_W^2} \right] C^{\phi WB} \\ & + \left[0.10 - 0.20 \log \frac{\mu^2}{M_W^2} \right] C^W - \left[0.11 - 0.04 \log \frac{\mu^2}{M_W^2} \right] C_{33}^{uB} + \left[0.71 - 0.28 \log \frac{\mu^2}{M_W^2} \right] C_{33}^{uW} \\ & - 0.01 C_{22}^{uW} - 0.01 C_{33}^{dW} + \dots , \end{aligned} \quad (\text{A.6})$$

$$\begin{aligned} \delta R_{h \rightarrow \gamma\gamma} \simeq & 0.18 (C_{1221}^{\ell\ell} - C_{11}^{\phi\ell(3)} - C_{22}^{\phi\ell(3)}) + 0.12 (C^{\phi\Box} - 2C^{\phi D}) \\ & - 0.01 (C_{22}^{e\phi} + 4C_{33}^{e\phi} + 5C_{22}^{u\phi} + 2C_{33}^{d\phi} - 3C_{33}^{u\phi}) \\ & - \left[48.04 - 1.07 \log \frac{\mu^2}{M_W^2} \right] C^{\phi B} - \left[14.29 - 0.12 \log \frac{\mu^2}{M_W^2} \right] C^{\phi W} + \left[26.17 - 0.52 \log \frac{\mu^2}{M_W^2} \right] C^{\phi WB} \\ & + \left[0.16 - 0.22 \log \frac{\mu^2}{M_W^2} \right] C^W + \left[2.11 - 0.84 \log \frac{\mu^2}{M_W^2} \right] C_{33}^{uB} + \left[1.13 - 0.45 \log \frac{\mu^2}{M_W^2} \right] C_{33}^{uW} \\ & - \left[0.03 - 0.01 \log \frac{\mu^2}{M_W^2} \right] C_{22}^{uB} - \left[0.01 - 0.00 \log \frac{\mu^2}{M_W^2} \right] C_{22}^{uW} + \left[0.03 - 0.01 \log \frac{\mu^2}{M_W^2} \right] C_{33}^{dB} \\ & - \left[0.02 - 0.01 \log \frac{\mu^2}{M_W^2} \right] C_{33}^{dW} + \left[0.02 - 0.00 \log \frac{\mu^2}{M_W^2} \right] C_{33}^{eB} - \left[0.01 - 0.00 \log \frac{\mu^2}{M_W^2} \right] C_{33}^{eW} + \dots . \end{aligned} \quad (\text{A.7})$$

A.2 Production channels

$$\delta R_{ggF} = 0.249 C_{33}^{d\phi} + 0.121 C^{\phi\square} - 0.303 C^{\phi D} - 0.129 C_{33}^{u\phi} - 0.0606 (C_{11}^{\phi\ell(3)} + C_{22}^{\phi\ell(3)} - C_{1221}^{\ell\ell}), \quad (\text{A.8})$$

$$\begin{aligned} \delta R_{\text{VBF}} = & -0.423 C_{11}^{\phi q(3)} - 0.347 C_{11}^{\phi q(1)} + 0.1005 C^{\phi \square} + 0.0826 C_{1221}^{\ell \ell} - 0.0670 C^{\phi W} \\ & - 0.0150 C^{\phi D} + 0.0126 C^{\phi WB} - 0.0107 C^{\phi B}, \end{aligned} \quad (\text{A.9})$$

$$\delta R_{Wh} = 1.950 C_{11}^{\phi q(3)} + 0.887 C^{\phi W} + 0.127 C^{\phi \square} + 0.0606 C_{1221}^{\ell\ell} - 0.0303 C^{\phi D}, \quad (\text{A.10})$$

$$\begin{aligned} \delta R_{Zh} = & 1.716 C_{11}^{\phi q(3)} + 0.721 C^{\phi W} + 0.426 C_{11}^{\phi u} - 0.173 C_{11}^{\phi q(1)} - 0.142 C_{11}^{\phi d} + 0.121 C^{\phi \square} \\ & + 0.0865 C^{\phi B} + 0.0375 C^{\phi D} + 0.314 C^{\phi WB} + 0.06045 C_{1221}^{\ell\ell}, \end{aligned} \quad (\text{A.11})$$

$$\delta R_{t\bar{t}h} = 0.121 C^{\phi\Box} - 0.122 C_{33}^{u\phi} - 0.0606 (C_{11}^{\phi\ell(3)} + C_{22}^{\phi\ell(3)} - C_{1221}^{\ell\ell}) - 0.0303 C^{\phi D}. \quad (\text{A.12})$$

B Model files and Wilson coefficients

As a complementary material we provide a csv file containing the two field models and several values of Wcs, observables and coupling values. More specifically the columns of the csv are the following

$$L1, L1bar, L2, L3, L4, L5, L6, L7, L8, L9, L10, L1L, L1Lbar, L1R, L1Rbar, L5L, L5R, \quad (B.2)$$

$$MSa, MSb, MFa, MFb, Y2, \quad (B.3)$$

$$CphiBox, CphiD, Cuphi33, Cdphi33, CphiB, CphiW, CphiWB, \quad (B.4)$$

$$dRhgangam, dSparam, dTparam, dRhbb, dRhWW, dRhtautau, dRhZZ, dRggF, \quad (B.5)$$

$$dRVBF, dRWh, dRZh, dRtth, dRhmu, dRhZgam, chi2min \} \quad (B.6)$$

In the first column is the model name as we discussed in Table 4. The next columns whose labels begin with L are the various coupling stemming from the Lagrangian of the model files and their corresponding values upon minimization of the χ^2 . Following are the relevant masses and the hypercharge for each model. Next, are the relevant Wcs, production and decay rates in this study and their values using the best-fit coupling from the previous columns. Finally, $dRhZgam$ contains the predictions to $\delta R_{h \rightarrow Z\gamma}$ for each respective model and for clarity we also mention in the last column the value of χ^2_{min} . Of course some models may not depend on all the quantities listed above. For example the two scalar models are not dependent of any fermion masses and vice versa. These values are treated as NaN values in the csv. One can load the csv in a nice Dataframe using python and the corresponding package pandas with the following lines of code,

```
import pandas as pd  
  
df = pd.read_csv("your-path-to-csv/all_models.csv")
```

Additionally to the csv we include all models files generated by SOLD, through its interface with the package MatachMakerEFT, for the two-field model cases presented above, in a zip file. In the model files one can make the connection between the couplings in the csv and the actual interactions in the Lagrangian.

References

- [1] **ATLAS** Collaboration, G. Aad *et al.*, “Observation of a new particle in the search for the Standard Model Higgs boson with the ATLAS detector at the LHC,” *Phys. Lett. B* **716** (2012) 1–29, [arXiv:1207.7214](https://arxiv.org/abs/1207.7214) [hep-ex].
- [2] **CMS** Collaboration, S. Chatrchyan *et al.*, “Observation of a New Boson at a Mass of 125 GeV with the CMS Experiment at the LHC,” *Phys. Lett. B* **716** (2012) 30–61, [arXiv:1207.7235](https://arxiv.org/abs/1207.7235) [hep-ex].
- [3] B. Henning, X. Lu, and H. Murayama, “How to use the Standard Model effective field theory,” *JHEP* **01** (2016) 023, [arXiv:1412.1837](https://arxiv.org/abs/1412.1837) [hep-ph].
- [4] I. Brivio and M. Trott, “The Standard Model as an Effective Field Theory,” *Phys. Rept.* **793** (2019) 1–98, [arXiv:1706.08945](https://arxiv.org/abs/1706.08945) [hep-ph].
- [5] G. Isidori, F. Wilsch, and D. Wyler, “The standard model effective field theory at work,” *Rev. Mod. Phys.* **96** no. 1, (2024) 015006, [arXiv:2303.16922](https://arxiv.org/abs/2303.16922) [hep-ph].
- [6] **ATLAS** Collaboration, M. Aaboud *et al.*, “Measurements of gluon-gluon fusion and vector-boson fusion Higgs boson production cross-sections in the $H \rightarrow WW^* \rightarrow e\nu\mu\nu$ decay channel in pp collisions at $\sqrt{s} = 13$ TeV with the ATLAS detector,” *Phys. Lett. B* **789** (2019) 508–529, [arXiv:1808.09054](https://arxiv.org/abs/1808.09054) [hep-ex].
- [7] **ATLAS** Collaboration, G. Aad *et al.*, “Measurement of the production cross section for a Higgs boson in association with a vector boson in the $H \rightarrow WW^* \rightarrow \ell\nu\ell\nu$ channel in pp collisions at $\sqrt{s} = 13$ TeV with the ATLAS detector,” *Phys. Lett. B* **798** (2019) 134949, [arXiv:1903.10052](https://arxiv.org/abs/1903.10052) [hep-ex].
- [8] **CMS** Collaboration, A. M. Sirunyan *et al.*, “Measurements of properties of the Higgs boson decaying to a W boson pair in pp collisions at $\sqrt{s} = 13$ TeV,” *Phys. Lett. B* **791** (2019) 96, [arXiv:1806.05246](https://arxiv.org/abs/1806.05246) [hep-ex].
- [9] **CMS** Collaboration, A. M. Sirunyan *et al.*, “Measurement of the inclusive and differential Higgs boson production cross sections in the leptonic WW decay mode at $\sqrt{s} = 13$ TeV,” *JHEP* **03** (2021) 003, [arXiv:2007.01984](https://arxiv.org/abs/2007.01984) [hep-ex].
- [10] **CMS** Collaboration, A. M. Sirunyan *et al.*, “Measurement and interpretation of differential cross sections for Higgs boson production at $\sqrt{s} = 13$ TeV,” *Phys. Lett. B* **792** (2019) 369–396, [arXiv:1812.06504](https://arxiv.org/abs/1812.06504) [hep-ex].
- [11] **ATLAS** Collaboration, G. Aad *et al.*, “Measurements of Higgs boson production and couplings in diboson final states with the ATLAS detector at the LHC,” *Phys. Lett. B* **726** (2013) 88–119, [arXiv:1307.1427](https://arxiv.org/abs/1307.1427) [hep-ex]. [Erratum: Phys.Lett.B 734, 406–406 (2014)].
- [12] **ATLAS** Collaboration, M. Aaboud *et al.*, “Measurements of Higgs boson properties in the diphoton decay channel with 36 fb^{-1} of pp collision data at $\sqrt{s} = 13$ TeV with the ATLAS detector,” *Phys. Rev. D* **98** (2018) 052005, [arXiv:1802.04146](https://arxiv.org/abs/1802.04146) [hep-ex].
- [13] **CMS** Collaboration, A. Tumasyan *et al.*, “A portrait of the Higgs boson by the CMS experiment ten years after the discovery.,” *Nature* **607** no. 7917, (2022) 60–68, [arXiv:2207.00043](https://arxiv.org/abs/2207.00043) [hep-ex].
- [14] **ATLAS** Collaboration, G. Aad *et al.*, “A detailed map of Higgs boson interactions by the ATLAS experiment ten years after the discovery,” *Nature* **607** no. 7917, (2022) 52–59, [arXiv:2207.00092](https://arxiv.org/abs/2207.00092) [hep-ex]. [Erratum: Nature 612, E24 (2022)].
- [15] **ATLAS, CMS** Collaboration, G. Aad *et al.*, “Evidence for the Higgs Boson Decay to a Z Boson and a Photon at the LHC,” *Phys. Rev. Lett.* **132** (2024) 021803, [arXiv:2309.03501](https://arxiv.org/abs/2309.03501) [hep-ex].

[16] X.-G. He, Z.-L. Huang, M.-W. Li, and C.-W. Liu, “The SM expected branching ratio for $h \rightarrow \gamma\gamma$ and an excess for $h \rightarrow Z\gamma$,” [arXiv:2402.08190 \[hep-ph\]](https://arxiv.org/abs/2402.08190).

[17] R. Boto, D. Das, J. C. Romao, I. Saha, and J. P. Silva, “New physics interpretations for nonstandard values of $h \rightarrow Z\gamma$,” [arXiv:2312.13050 \[hep-ph\]](https://arxiv.org/abs/2312.13050).

[18] T. T. Hong, V. K. Le, L. T. T. Phuong, N. . C. Hoi, N. T. K. Ngan, and N. H. T. Nha, “Decays of Standard Model like Higgs boson $h \rightarrow \gamma\gamma, Z\gamma$ in a minimal left-right symmetric model,” [arXiv:2312.11045 \[hep-ph\]](https://arxiv.org/abs/2312.11045).

[19] D. Barducci, L. Di Luzio, M. Nardecchia, and C. Toni, “Closing in on new chiral leptons at the LHC,” *JHEP* **12** (2023) 154, [arXiv:2311.10130 \[hep-ph\]](https://arxiv.org/abs/2311.10130).

[20] C. Grojean, G. Guedes, J. Roosmale Nepveu, and G. M. Salla, “A log story short: running contributions to radiative Higgs decays in the SMEFT,” [arXiv:2405.20371 \[hep-ph\]](https://arxiv.org/abs/2405.20371).

[21] S. Israr and M. Rehman, “Higgs Decay to $Z\gamma$ in the Minimal Supersymmetric Standard Model and Its Nonholomorphic Extension,” [arXiv:2407.01210 \[hep-ph\]](https://arxiv.org/abs/2407.01210).

[22] M. K. Gaillard, “The Effective One Loop Lagrangian With Derivative Couplings,” *Nucl. Phys. B* **268** (1986) 669–692.

[23] O. Cheyette, “Effective Action for the Standard Model With Large Higgs Mass,” *Nucl. Phys. B* **297** (1988) 183–204.

[24] Z. Zhang, “Covariant diagrams for one-loop matching,” *JHEP* **05** (2017) 152, [arXiv:1610.00710 \[hep-ph\]](https://arxiv.org/abs/1610.00710).

[25] T. Cohen, X. Lu, and Z. Zhang, “Functional Prescription for EFT Matching,” *JHEP* **02** (2021) 228, [arXiv:2011.02484 \[hep-ph\]](https://arxiv.org/abs/2011.02484).

[26] A. Drozd, J. Ellis, J. Quevillon, and T. You, “The Universal One-Loop Effective Action,” *JHEP* **03** (2016) 180, [arXiv:1512.03003 \[hep-ph\]](https://arxiv.org/abs/1512.03003).

[27] S. A. R. Ellis, J. Quevillon, T. You, and Z. Zhang, “Mixed heavy–light matching in the Universal One-Loop Effective Action,” *Phys. Lett. B* **762** (2016) 166–176, [arXiv:1604.02445 \[hep-ph\]](https://arxiv.org/abs/1604.02445).

[28] J. Fuentes-Martin, J. Portoles, and P. Ruiz-Femenia, “Integrating out heavy particles with functional methods: a simplified framework,” *JHEP* **09** (2016) 156, [arXiv:1607.02142 \[hep-ph\]](https://arxiv.org/abs/1607.02142).

[29] S. A. R. Ellis, J. Quevillon, T. You, and Z. Zhang, “Extending the Universal One-Loop Effective Action: Heavy-Light Coefficients,” *JHEP* **08** (2017) 054, [arXiv:1706.07765 \[hep-ph\]](https://arxiv.org/abs/1706.07765).

[30] B. Summ and A. Voigt, “Extending the Universal One-Loop Effective Action by Regularization Scheme Translating Operators,” *JHEP* **08** (2018) 026, [arXiv:1806.05171 \[hep-ph\]](https://arxiv.org/abs/1806.05171).

[31] M. Krämer, B. Summ, and A. Voigt, “Completing the scalar and fermionic Universal One-Loop Effective Action,” *JHEP* **01** (2020) 079, [arXiv:1908.04798 \[hep-ph\]](https://arxiv.org/abs/1908.04798).

[32] B. Summ, *One Formula To Match Them All: The Bispinor Universal One-Loop Effective Action*. PhD thesis, RWTH Aachen U., 2020. [arXiv:2103.02487 \[hep-ph\]](https://arxiv.org/abs/2103.02487).

[33] S. A. R. Ellis, J. Quevillon, P. N. H. Vuong, T. You, and Z. Zhang, “The Fermionic Universal One-Loop Effective Action,” *JHEP* **11** (2020) 078, [arXiv:2006.16260 \[hep-ph\]](https://arxiv.org/abs/2006.16260).

[34] A. Angelescu and P. Huang, “Integrating Out New Fermions at One Loop,” *JHEP* **01** (2021) 049, [arXiv:2006.16532 \[hep-ph\]](https://arxiv.org/abs/2006.16532).

[35] J. Fuentes-Martín, A. Palavrić, and A. E. Thomsen, “Functional matching and renormalization group equations at two-loop order,” *Phys. Lett. B* **851** (2024) 138557, [arXiv:2311.13630 \[hep-ph\]](https://arxiv.org/abs/2311.13630).

[36] T. Cohen, X. Lu, and Z. Zhang, “STrEAMlining EFT Matching,” *SciPost Phys.* **10** no. 5, (2021) 098, [arXiv:2012.07851 \[hep-ph\]](https://arxiv.org/abs/2012.07851).

[37] J. Fuentes-Martin, M. König, J. Pagès, A. E. Thomsen, and F. Wilsch, “SuperTracer: A Calculator of Functional Supertraces for One-Loop EFT Matching,” *JHEP* **04** (2021) 281, [arXiv:2012.08506 \[hep-ph\]](https://arxiv.org/abs/2012.08506).

[38] S. Das Bakshi, J. Chakrabortty, and S. K. Patra, “CoDEx: Wilson coefficient calculator connecting SMEFT to UV theory,” *Eur. Phys. J. C* **79** no. 1, (2019) 21, [arXiv:1808.04403 \[hep-ph\]](https://arxiv.org/abs/1808.04403).

[39] J. Fuentes-Martín, M. König, J. Pagès, A. E. Thomsen, and F. Wilsch, “A proof of concept for matchete: an automated tool for matching effective theories,” *Eur. Phys. J. C* **83** no. 7, (2023) 662, [arXiv:2212.04510 \[hep-ph\]](https://arxiv.org/abs/2212.04510).

[40] A. Carmona, A. Lazopoulos, P. Olgoso, and J. Santiago, “Matchmakereft: automated tree-level and one-loop matching,” *SciPost Phys.* **12** no. 6, (2022) 198, [arXiv:2112.10787 \[hep-ph\]](https://arxiv.org/abs/2112.10787).

[41] G. Guedes, P. Olgoso, and J. Santiago, “Towards the one loop IR/UV dictionary in the SMEFT: One loop generated operators from new scalars and fermions,” *SciPost Phys.* **15** no. 4, (2023) 143, [arXiv:2303.16965 \[hep-ph\]](https://arxiv.org/abs/2303.16965).

[42] A. Dedes and K. Mantzaropoulos, “Universal scalar leptoquark action for matching,” *JHEP* **11** (2021) 166, [arXiv:2108.10055 \[hep-ph\]](https://arxiv.org/abs/2108.10055).

[43] B. Grzadkowski, M. Iskrzynski, M. Misiak, and J. Rosiek, “Dimension-Six Terms in the Standard Model Lagrangian,” *JHEP* **10** (2010) 085, [arXiv:1008.4884 \[hep-ph\]](https://arxiv.org/abs/1008.4884).

[44] J. de Blas, J. C. Criado, M. Perez-Victoria, and J. Santiago, “Effective description of general extensions of the Standard Model: the complete tree-level dictionary,” *JHEP* **03** (2018) 109, [arXiv:1711.10391 \[hep-ph\]](https://arxiv.org/abs/1711.10391).

[45] A. Dedes, M. Paraskevas, J. Rosiek, K. Suxho, and L. Trifyllis, “The decay $h \rightarrow \gamma\gamma$ in the Standard-Model Effective Field Theory,” *JHEP* **08** (2018) 103, [arXiv:1805.00302 \[hep-ph\]](https://arxiv.org/abs/1805.00302).

[46] A. Dedes, K. Suxho, and L. Trifyllis, “The decay $h \rightarrow Z\gamma$ in the Standard-Model Effective Field Theory,” *JHEP* **06** (2019) 115, [arXiv:1903.12046 \[hep-ph\]](https://arxiv.org/abs/1903.12046).

[47] S. Descotes-Genon, A. Falkowski, M. Fedele, M. González-Alonso, and J. Virto, “The CKM parameters in the SMEFT,” *JHEP* **05** (2019) 172, [arXiv:1812.08163 \[hep-ph\]](https://arxiv.org/abs/1812.08163).

[48] A. Dedes, W. Materkowska, M. Paraskevas, J. Rosiek, and K. Suxho, “Feynman rules for the Standard Model Effective Field Theory in R_ξ -gauges,” *JHEP* **06** (2017) 143, [arXiv:1704.03888 \[hep-ph\]](https://arxiv.org/abs/1704.03888).

[49] **Particle Data Group** Collaboration, R. L. Workman *et al.*, “Review of Particle Physics,” *PTEP* **2022** (2022) 083C01.

[50] G. T. Bodwin and H. S. Chung, “New method for fitting coefficients in standard model effective theory,” *Phys. Rev. D* **101** no. 11, (2020) 115039, [arXiv:1912.09843 \[hep-ph\]](https://arxiv.org/abs/1912.09843).

[51] X.-X. Li, Z. Ren, and J.-H. Yub, “Complete tree-level dictionary between simplified BSM models and SMEFT $d \leq 7$ operators,” *Phys. Rev. D* **109** no. 9, (2024) 095041, [arXiv:2307.10380 \[hep-ph\]](https://arxiv.org/abs/2307.10380).

[52] S. Das Bakshi, S. Dawson, D. Fontes, and S. Homiller, “Relevance of one-loop SMEFT matching in the 2HDM,” [arXiv:2401.12279 \[hep-ph\]](https://arxiv.org/abs/2401.12279).